JOURNAL OF CATALYSIS 152, 130–136 (1995)

Characterization of γ-Alumina-Supported Vanadium Oxide Monolayers

A. W. Stobbe-Kreemers,* G. C. van Leerdam,† J.-P. Jacobs,†
H. H. Brongersma,† and J. J. F. Scholten*

*Department of Chemical Engineering, Delft University of Technology, Julianalaan 136, 2628 BL Delft, The Netherlands; and †Faculty of Physics and Schuit Institute of Catalysis, Eindhoven University of Technology, P.O. Box 513, 5600 MB Eindhoven, The Netherlands

Received January 4, 1994; revised March 28, 1994

The structure and properties of vanadium oxide deposited on γ-alumina at submonolayer coverage have been investigated. Textural analysis, electron microscopy, and low energy ion scattering (LEIS) show that, for loadings up to at least 3.4 V/nm^2, the vanadium oxide is present as a highly dispersed phase. LEIS experiments show that the development of the vanadium oxide monolayer proceeds in three steps. In the first step vanadium oxide is molecularly dispersed on γ-alumina as isolated monomeric and dimeric species. Above approximately 1.5 V/nm^2 a second layer of vanadium oxide is formed on top of the dimeric species, resulting in the formation of oligomeric species. At coverages above 2.5 V/nm^2 these small oligomeric species grow into polymeric vanadium oxide chains. TPR experiments show that reduction of these polymeric species proceeds at lower temperatures than reduction of the monomeric species, probably as a result of the weakening of the vanadium–oxygen bond.

INTRODUCTION

Wacker oxidation is the selective oxidation of alkenes to aldehydes or ketones, catalyzed by palladium(II) complexes (1, 2). Examples are the oxidation of ethene to acetaldehyde and of 1-butene to butanone. A new heterogeneous catalyst for Wacker oxidation has been developed by Scholten and co-workers (3), consisting of a supported vanadium oxide monolayer on which a palladium(II) salt is deposited.

During the reaction, Pd^{2+} is reduced to Pd(0) by the alkene. In order to be able to run the reaction continuously, Pd^{2+} is regenerated *in situ* by a redox compound. In the original homogeneously catalyzed process copper(II) chloride is used for this purpose, but in the new heterogeneous catalyst $CuCl_2$ is replaced by vanadium oxide. The complete process, including the regeneration of the Pd^{2+} and of the redox compound, can be described by the following three reactions:

$$Pd^{2+} + H_2O + C_2H_4 \rightleftarrows Pd(0) + C_2H_4O + 2H^+ \quad [1]$$

$$Pd(0) + V_2O_5 + 2H^+ \rightleftarrows Pd^{2+} + H_2V_2O_5 \quad [2]$$

$$H_2V_2O_5 + \tfrac{1}{2}O_2 \rightarrow V_2O_5 + H_2O \quad [3]$$

In Eqs. 2 and 3 the stoichiometry of the vanadium bronze $H_xV_2O_5$ is written with $x = 2$, but other stoichiometries are possible as well.

Because of their redox properties, supported vanadium oxide catalysts are widely used as selective catalysts in both oxidation and reduction reactions (4). For instance, vanadium oxide on titania (anatase) is used in *o*-xylene and methanol oxidation as well as in the selective catalytic reduction of NO_x (4). The properties of supported vanadium oxide catalysts strongly depend on the vanadium oxide coverage and the best results are often obtained with catalysts possessing a monolayer coverage. This is also the case for the heterogeneous Wacker oxidation catalyst. It turns out that the vanadium oxide redox system is applicable only when the coverage does not exceed a monolayer (3).

The formation of vanadium oxide monolayers has been described in the literature only since the last decade. Many studies have been undertaken to gain insight into the formation and properties of these monolayers (5–12). As a result of these studies, it is now generally accepted that at low loadings vanadium oxide forms a highly dispersed monolayer phase on various supports, such as, e.g., γ-alumina, titania (anatase), and zirconia. At monolayer coverage a strong interaction between the support and the vanadium oxide phase exists. Due to this strong interaction the structure and the reactivity of the vanadium oxide are modified. This is displayed, *inter alia*, in an increased reducibility of the supported vanadium oxide (4, 5, 10, 13–15).

This paper deals with the preparation and characterization of vanadium oxide monolayers on γ-alumina. Samples of vanadium oxide on γ-alumina, loaded up to monolayer coverage, have been investigated using several characterization techniques, such as textural analysis and

0021-9517/95 $6.00

electron microscopy. Studies of supported vanadium oxide catalysts, described in the literature, often make use of characterization techniques, such as ^{51}V NMR, Laser Raman, and EXAFS. Low energy ion scattering (LEIS) is also a very suitable technique for investigating the structure of monolayer catalysts (16). Therefore, this technique is used here to study vanadium oxide on γ-alumina. The reducibility of the vanadium oxide species in the samples has been investigated using temperature programmed reduction (TPR).

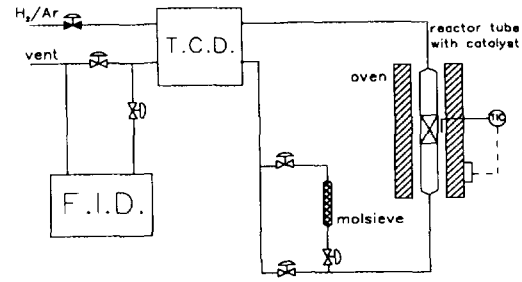

FIG. 1. Schematic drawing of temperature programmed reduction flow equipment. T.C.D. is the thermal conductivity detector and F.I.D. is the flame ionization detector.

EXPERIMENTAL

A series of samples of vanadium oxide on γ-alumina was prepared. γ-Al_2O_3 extrudates (Akzo, type 000-3P), BET surface area 269 m^2/g, were used as support material. Before use, the extrudates were crushed and sieved, and the fraction of 400 to 625 μm was used for catalyst preparation. Catalysts were prepared batchwise by contacting the γ-alumina particles with an aqueous NH_4VO_3 solution (Merck, analytical grade, 10 g/dm^3, pH = 4) at 293 or 343 K. A series of samples with increasing vanadium oxide coverage was prepared by varying the contact time. Subsequently, the samples were taken from the solution and washed with demineralized water. Samples were then dried at 350 K for 16 h and calcined in air at 675 K for 4 h. The vanadium oxide content was determined by titration with Fe^{2+}, applying the method described by Walden *et al.* (17).

The point of zero charge (PZC) of several samples and of pure γ-alumina and V_2O_5 (Aldrich, 99.6+%) was estimated according to the procedure described by Noh and Schwarz (18). Various amounts of the sample were added to demineralized water (under N_2) and the resulting equilibrium pH of the suspension was measured after 24 h. This was done for 0.1, 1, 5, 10, and 20 wt.% of sample. The PZC of the samples was estimated from the plot of the pH of the suspension versus the logarithm of wt.% of sample by extrapolating the curve to infinite mass. Pore volume distributions of the samples (after pretreatment at 423 K for 12 h in oxygen) were determined from the capillary condensation of nitrogen at 77 K using the Broekhoff–de Boer method (19).

Temperature programmed reduction was performed using the equipment shown in Fig. 1. Approximately 100–200 mg of sample was loaded into the quartz reactor tube and heated at a rate of 0.17 K/s in a flow of 0.5 cm^3 (STP)/s of 66% H_2 in argon. Hydrogen consumption was detected with a thermal conductivity detector (TCD). The sensitivity of the TCD for hydrogen was calibrated by means of reduction of CuO to Cu.

Low energy ion scattering experiments were performed with the LEIS apparatus NODUS outlined elsewhere (20). Monoenergetic ions were produced in a Leybold ion source and directed onto the target. A cylindrical mirror analyzer selects ions scattered at an angle of 142°. The energy spectrum of the selected ions was recorded. The differential pumping system ensured that the background pressure increased from 5×10^{-8} to 1×10^{-6} Pa only when the ion beam was used. This increase was mainly due to helium.

The samples were powdered and pressed in tantalum discs and then mounted onto the target holders. Before entering the UHV chamber the samples were dehydrated by heating in oxygen (10^3 Pa) at 500 K for 15 min, followed by evacuation for 10 min. After this pretreatment the samples were inserted into the UHV chamber and placed on a carousel that can hold 12 samples. This carousel system ensured identical experimental conditions for a series of samples, enabling a direct comparison of the samples. Typical experimental conditions used a beam current of 200 nA, a $^4He^+$ probe, a beam diameter between 0.5 and 5 mm, depending on the desired sputtering rate, and a primary ion energy of 3 keV. Surface charging effects were eliminated by flooding the surface with low energy electrons from a ring-shaped neutralizing system, which ensures flooding from all sides. To retard destruction of the samples, a light ion (^4He) is used and the ion flux is kept as low as possible. Time-dependent measurements show that the influence of damage by the ion beam on the present data can be neglected.

RESULTS AND DISCUSSION

Samples with increasing vanadium oxide coverage were prepared by varying the impregnation contact time. Figure 2 shows the uptake of vanadium oxide as a function of contact time at 293 and 343 K. At both 293 and 343 K adsorption of vanadium species initially proceeds quickly. At room temperature vanadium oxide loadings of approximately 1.6 V/nm^2 are reached within 1 h. Beyond this time, the further adsorption of vanadium species proceeds only slowly. After an additional 5 h the vanadium oxide coverage has increased by only about 0.1 V/nm^2. At 343

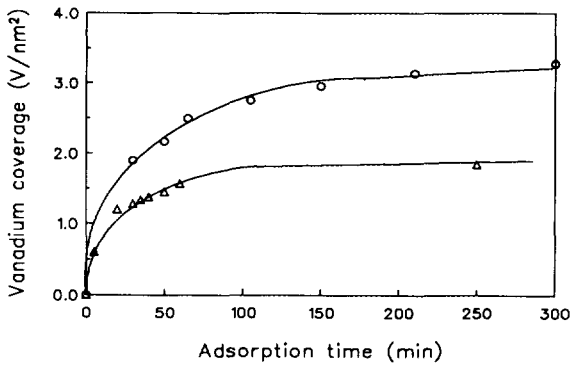

FIG. 2. Vanadium oxide adsorption on γ-alumina at 293 K (△) and 343 K (○) from a 0.085 *M* NH_4VO_3 solution at pH = 4.

K, however, the adsorption process immediately proceeds to higher vanadium oxide loadings and an equilibrium coverage of 3.4 V/nm² is reached, in good accordance with the value of 3.3 V/nm² reported by Le Coustumier *et al.* (21).

The nature of the vanadium oxide species in solution strongly depends on the pH and the concentration (23). The degree of polymerization increases with increasing concentration and decreasing pH. Under the conditions used in the experiments of Fig. 2, i.e., at pH = 4 and at a vanadium concentration of 0.085 *M*, vanadium is predominantly present in the form of negatively charged decavanadate species $V_{10}O_{27}(OH)^{5-}$ (23).

The charge of the γ-alumina surface in the solution is determined both by the PZC of the alumina and by the pH of the solution. The PZC is defined as the pH at which the net charge of the oxide surface is zero. At a pH below the PZC the surface is positively charged, whereas above the PZC the net surface charge is negative. The PZC of γ-alumina has been determined by extrapolation of the curve shown in Fig. 3A to infinite mass. Thus a PZC value of 7.4 is found, in good agreement with the values between 6 and 8 reported in the literature (18, 24, 25). It can be concluded that under the preparation conditions used, i.e., at pH = 4, the surface of the γ-alumina is positively

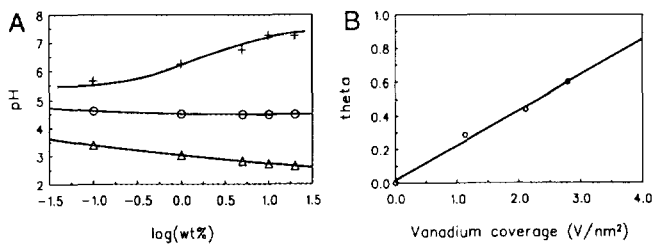

FIG. 3. (A) Determination of PZC of γ-alumina (+), V_2O_5 (△), and 11.3 wt.% V_2O_5 on γ-alumina (○). (B) Vanadium oxide coverage θ (calculated from PZC) as a function of the vanadium oxide loading.

charged and will exhibit a strong affinity for the negatively charged decavanadate ions in the solution.

Since it is impossible to remove the adsorbed vanadium species by washing the samples with demineralized water it is concluded that the adsorption process is irreversible. This points to a strong interaction being present between the adsorbed vanadium oxide species and the γ-alumina surface already in the noncalcined samples, as is confirmed by Le Coustumier *et al.* (21) and Lapina *et al.* (22). Most probably, the adsorption process is a result of an electrostatic interaction between the vanadium oxide species in the solution and the γ-alumina surface, followed by a reaction between the adsorbed vanadium oxide species and γ-alumina surface groups. The increased adsorption rate at higher temperature is probably a result of a faster reaction of the vanadium oxide species with the γ-alumina surface.

Figure 3A also shows the PZC determination for pure vanadium pentaoxide and for a calcined sample of 11.3 wt.% vanadium oxide on γ-alumina. The PZC of vanadium pentaoxide is found to be 2.6. The PZC of 11.3 wt.% vanadium oxide on γ-alumina sample lies between the PZC values of the pure support and the pure vanadium pentaoxide and reflects the surface composition. Assuming that the PZC of monolayer vanadium oxide is equal to the PZC of crystalline vanadium pentaoxide, the vanadium oxide coverage θ can be estimated according to:

$$PZC_{sample} = \theta \cdot PZC_{V_2O_5} + (1 - \theta) \cdot PZC_{\gamma\text{-alumina}}. \quad [4]$$

From the PZC's of several vanadium-oxide-containing samples θ has been calculated and the results are depicted in Fig. 3B. A linear relation between the vanadium oxide loading and the coverage of the samples is found. Moreover, from Fig. 3B it can be estimated that the γ-alumina surface will be completely covered by the vanadium oxide at approximately 5 V/nm². This indicates that the vanadium oxide is deposited on the γ-alumina as a highly dispersed phase. However, this is only an indication, and no conclusions can be drawn regarding the structure of this vanadium oxide phase.

The formation of a highly dispersed vanadium oxide layer is confirmed by the textural analysis of the γ-alumina before and after vanadium oxide deposition. Figure 4 shows the pore size distribution of the pure γ-alumina support and of a 14.1 wt.% vanadium oxide on γ-alumina sample. The shape of the pore size distribution is almost identical for the two samples, indicating that no blocking of pores has occurred during the vanadium oxide deposition. The average pore size of the vanadium-containing sample, however, is a few angstroms smaller than that of the pure support. A thin uniform layer of vanadium oxide is formed inside the pores, for which an average layer thickness of approximately 3 Å is calculated.

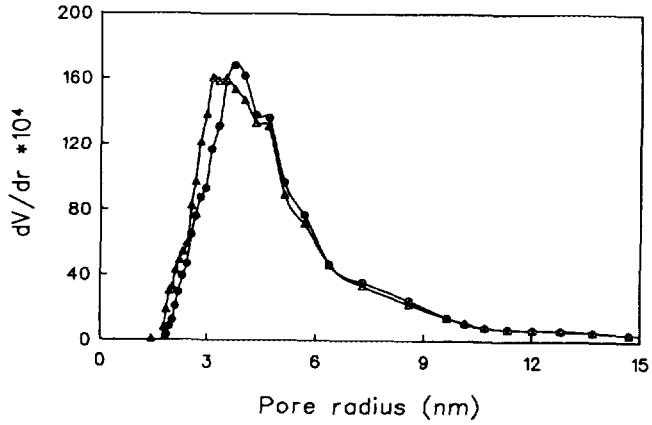

FIG. 4. Differential pore volume distribution of pure γ-alumina (●) and of a 14.1 wt.% vanadium oxide on γ-alumina sample (△). Curves are normalized to 1 g γ-alumina.

γ-Alumina and vanadium-oxide-containing samples have been investigated with scanning electron microscopy. No vanadium oxide particles could be detected in the vanadium-containing samples and EDX analysis showed that the vanadium oxide is homogeneously distributed over the γ-alumina surface. The absence of crystalline vanadium oxide phases has been confirmed by X-ray diffraction as well.

The above results show that vanadium oxide forms a molecularly dispersed layer on the γ-alumina surface, which is confirmed by many other authors (4, 5, 9–11). The structure of this layer has been further investigated with LEIS. Peak heights are taken as a measure for scattered intensities, but the same results are obtained if areas are used instead. LEIS spectra were recorded for a series of samples with increasing vanadium oxide content. Figure 5 shows the vanadium, oxygen, and aluminum peak heights as a function of the vanadium oxide coverage.

Three stages can be distinguished in the formation of

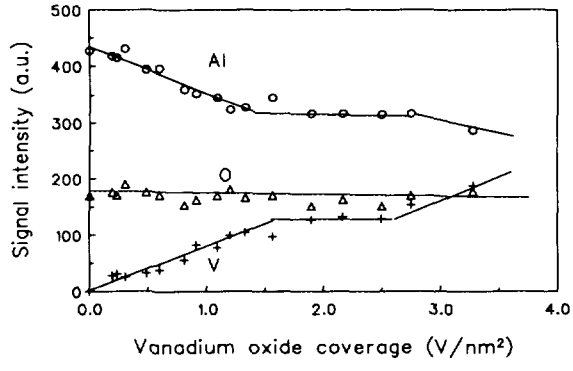

FIG. 5. Vanadium, oxygen, and aluminum peak heights, measured in LEIS experiments, as a function of the vanadium oxide loading of the samples.

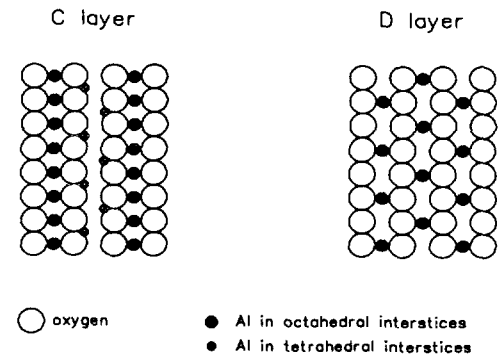

FIG. 6. C and D layers of the (110) crystal face of γ-alumina spinel.

the vanadium oxide layer. The first stage, from 0 to 1.5 V/nm², is characterized by an increase of the vanadium signal and a simultaneous decrease of the aluminum signal. Both signals change linearly with the vanadium content, indicating that vanadium oxide is molecularly dispersed on the γ-alumina surface. As the deposited vanadium oxide covers the γ-alumina surface, it shields part of the aluminum ions from detection, resulting in the observed decrease of the aluminum signal.

Above 1.5 V/nm² the vanadium signal is found to be constant up to a coverage of approximately 2.5 V/nm². The fact that the vanadium content of the samples increases while the vanadium signal remains constant can be explained only by assuming that a second layer of vanadium oxide is formed. The additional vanadium is deposited on top of the vanadium already present in the sample. This is also confirmed by the constant aluminum signal, which indicates that no additional γ-alumina surface is covered during this stage.

Above 2.5 V/nm² the vanadium signal again starts to increase with the vanadium oxide loading of the samples. The simultaneous decrease of the aluminum signal shows that the vanadium is deposited on thus far uncovered parts of the γ-alumina surface in this third stage. The oxygen signal is approximately constant over the complete range of vanadium oxide loadings. This points to an epitaxial growth of vanadium oxide on the γ-alumina surface, thereby extending the oxygen lattice of the γ-alumina.

γ-Alumina possesses a defect spinel structure (26–28). There has been discussion in the literature about the preferentially exposed crystal planes of γ-alumina (26–28). The low-index planes (001), (110), and (111) are the most probable ones but no conclusive answer has been given. Van Leerdam (29), from his LEIS study of several aluminas, found indications that only one or two crystal planes are preferentially exposed. His results suggest that for his γ-alumina the D layer of the (110) face is predominant. This D layer, shown in Fig. 6, is characterized by low

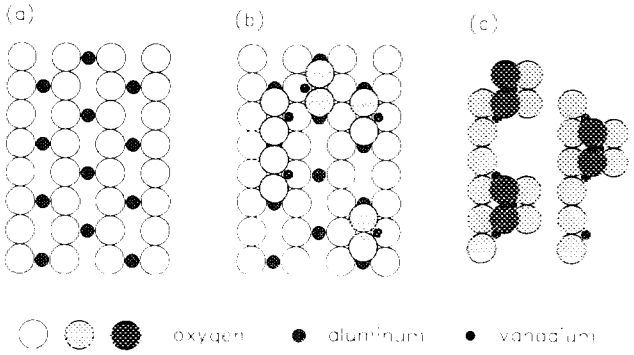

FIG. 7. Model for the formation of a vanadium oxide monolayer on γ-alumina. (a) D layer of the (110) face of the γ-alumina spinel, (b) extension of the D layer by vanadium oxide species, and (c) formation of a second layer of vanadium oxide.

aluminum content of the surface and exclusive exposure of octahedral interstices, filled with aluminum. Extension of the spinel structure, starting from this D layer, results in the formation of the C layer, also depicted in Fig. 6. This C layer consists of rows of oxygen and alternating rows of tetrahedral and octahedral interstices. Results on other spinel structures also show a preferential exposure of crystal planes which contain only octahedral sites (30).

Nowińska and Więckowski (31), in an EPR study on vanadium oxide on γ-alumina, concluded from a geometric analysis of the crystal planes of γ-alumina that vanadyl species could be located either on the (100) plane of γ-alumina or on the C and D layers of the (110) plane. Regarding the LEIS results on spinels (29, 30), location on the D layer of γ-alumina is most likely. The model for the structure of the supported vanadium oxide monolayer catalyst presented here is hence based on the assumption of predominant exposure of the D layer of the (110) face of γ-alumina.

Epitaxial growth of the deposited vanadium oxide on this D layer, depicted in Fig. 7a, results in the formation of a C layer. In this C layer vanadium could be deposited in either the tetrahedral or the octahedral interstices of the layer. The results of many characterization studies reported in the literature show that at low coverage vanadium is found to be tetrahedrally surrounded on the γ-alumina surface (6, 8, 9, 12). Therefore, the vanadium is presumed to be exclusively deposited in the tetrahedral interstices of the C layer, as shown in Fig. 7b. This figure clearly shows that the deposited vanadium oxide species shield the aluminum atoms of the underlying D layer from detection, resulting in the decrease of the aluminum signal (see Fig. 5).

Complete occupation of the tetrahedral positions of the C layer would result in a surface coverage of approximately 4.6 V/nm^2. The LEIS experiment, however, shows that only 1.5 V/nm^2 are deposited at this stage, resulting in occupation of one-third of the tetrahedral interstices. Therefore, most of the particles formed at this stage are isolated monomeric or dimeric species.

The next stage of the development of the monolayer is characterized by the formation of a second layer. Vanadium oxide is deposited on top of the mono- and dimeric species developed at the first stage, and oligomeric species are formed. Figure 7c shows that the vanadium atoms deposited at the first stage are shielded by the vanadium atoms on top of these oligomeric species. In the literature the formation of polymeric metavanadate chains is reported at intermediate loadings (4–6, 9, 22). The oligomeric particles presented in this model can also be regarded as $(VO_3)_n$ chains with a low degree of polymerization. Moreover, the model proposed by Bergeret *et al.* (32) of chains of corner-linked tetrahedra of vanadium oxide shows a strong resemblance to the model in Fig. 7c. The vanadium–vanadium distances in their model based on RED measurements are almost equal to the distances in the model in Fig. 7c.

The first two stages of monolayer formation result in the formation of rows of oligomeric species on the γ-alumina surface. At loadings above 2.5 V/nm^2 the alumina surface is further covered by vanadium oxide. The simultaneous decrease in aluminum signal and increase in vanadium signal point to the deposition of vanadium on thus far uncovered parts of the surface, either connecting the oligomeric particles already formed or cross-linking them by filling the octahedral interstices of the new C layer, thus forming three-dimensional vanadium oxide polymers. Other characterization studies have indeed shown that at increasing vanadium loading three-dimensional decavanadate-like structures are formed at the surface (4–6, 9). Moreover, our LEIS results are confirmed by the results of Eberhardt *et al.* (33).

The existence of different types of vanadium species on the γ-alumina support is also confirmed by the results of TPR experiments. Figure 8A shows the TPR profiles of several samples used in the LEIS experiments. Vanadium oxide reduction is found to proceed between 575 and 875 K. The temperature of maximum reduction rate (T_{max}) appears to vary with the vanadium oxide coverage. In Fig. 8B T_{max} values are plotted as a function of the vanadium oxide coverage of the samples and are found to decrease by almost 30 K over the range from 1 to 3.3 V/nm^2. The change in reduction temperature is especially large at low loadings.

This difference in reducibility is probably caused by the changing structure of the vanadium species. At low coverages of the γ-alumina surface isolated monomeric and dimeric species of vanadium oxide are most abundant. At loadings above 1.5 V/nm^2 these isolated species grow into larger oligomeric species, in which part of the vanadium possesses a different surrounding. At even higher

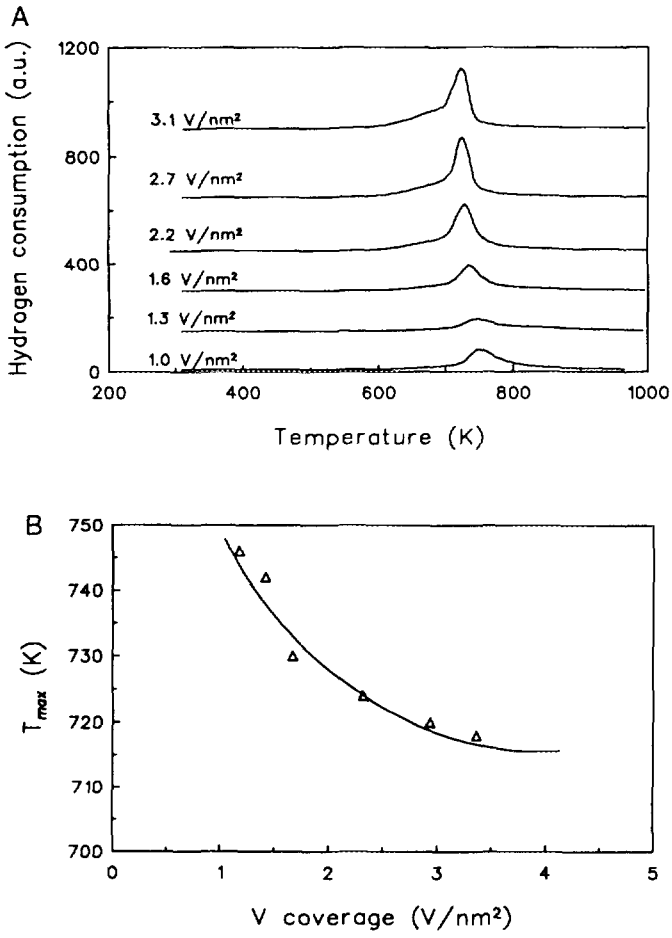

FIG. 8. The effect of the vanadium oxide coverage on the reduction behavior. (A) TPR profiles at various vanadium oxide coverage. The profiles are normalized to 200 mg sample weight. (B) Temperature of maximum reduction rate as a function of the vanadium oxide coverage.

vanadium oxide loadings, vanadium oxide polymers are formed. The largest change in properties of the vanadium oxide species is of course expected when the isolated species transform into oligomeric species. Both the size of the species and the vanadium surrounding change at that point and this is displayed in a large shift in reduction temperature in this region. Since T_{max} decreases with the vanadium oxide loading, reduction appears to be enhanced by an increased degree of polymerization of the vanadium oxide. Bonné (34) reported a similar decrease in the vanadium oxide reduction temperature with increasing vanadium oxide coverage. He also showed, by means of XPS analysis, that upon increasing the vanadium oxide coverage the binding energy of the vanadium atoms decreases. This decrease in binding energy is probably caused by a weakening of the vanadium–oxygen bond strength with increasing degree of polymerization of the vanadium oxide. The decrease in vanadium–oxygen bond strength is reflected in the lower reduction temperature.

CONCLUSIONS

Vanadium oxide is irreversibly adsorbed on the γ-alumina surface from acidic ammonium metavanadate solutions. Negatively charged decavanadate species are adsorbed at the positively charged γ-alumina surface. At pH = 4 and a vanadium concentration of 0.085 *M*, this adsorption process results in an equilibrium surface coverage of 3.4 V/nm^2.

Drying and calcination of the samples results in the formation of a highly dispersed vanadium oxide layer on the γ-alumina support. Textural analysis and electron microscopy experiments show that vanadium oxide is uniformly distributed over the γ-alumina surface. Determination of the point of zero charge of the vanadium-oxide-containing samples reveals that the PZC is indicative for the surface composition of the samples. The fraction of the surface covered with vanadium oxide, θ, is found to increase linearly with the vanadium content of the samples. Complete coverage of the γ-alumina surface, i.e., $\theta = 1$, is estimated to correspond with a vanadium loading of approximately 5 V/nm^2.

LEIS experiments show that the formation of the monolayer proceeds in three stages. In the first stage monomeric and dimeric vanadium oxide species are deposited at tetrahedral positions on the γ-alumina surface. In the next stage a second layer of vanadium is deposited on top of these species, resulting in the formation of two-layered oligomeric species. A further increase of the vanadium oxide loading results in the formation of polymeric chains of vanadium oxide on the γ-alumina surface. The results from the LEIS experiments are in good agreement with results reported in the literature.

TPR reveals that the reduction temperature of the supported vanadium oxide decreases with increasing vanadium oxide content of the samples. Reduction of polymeric vanadium oxide species, therefore, appears to be easier than reduction of monomeric vanadium oxide species.

ACKNOWLEDGMENTS

The work described in this article was supported by the Netherlands Foundation for Chemical Research (SON), with financial aid of the Netherlands Organization for Scientific Research (NWO).

REFERENCES

1. Smidt, J., Hafner, W., Jira, R., Sedlmeier, J., Sieber, R., Ruttinger, R., and Kojer, H., *Agnew. Chem.* **71,** 176 (1959).
2. Henry, P. M., *J. Am. Chem. Soc.* **86,** 3246 (1964).
3. Van der Steen, P. J., Ph.D. thesis, Chap. 3, Delft University of Technology, 1987 [in Dutch]; Van der Heide, E., Ph.D. thesis, Delft University of Technology, 1990; Van der Heide, E., de Wind, M., Gerritsen, A. W., and Scholten, J. J. F., *in* "Proceedings, 9th International Congress on Catalysis, Calgary, 1988" (M. J. Phillips and

M. Ternan, Eds.), Vol. IV, p. 1648. Chem. Institute of Canada, Ottawa, 1988.
4. Bond, G. C., and Tahir, S. F., *Appl. Catal.* **71,** 1 (1991).
5. Haber, J., Kozłowska, A., and Kozłowski, R., *in* "Proceedings, 9th International Congress on Catalysis, Calgary, 1988" (M. J. Phillips and M. Ternan, Eds.), Vol. III, p. 1481. Chem. Institute of Canada, Ottawa, 1988; Haber, J., Kozłowska, A., and Kozłowski, R., *J. Catal.* **102,** 52 (1986).
6. Eckert, H., and Wachs, I. E., *J. Phys. Chem.* **93,** 6796 (1989).
7. Wachs, I.E., Jeng, J. M., and Hardcastle, F. D., *Solid State Ionics* **32/33,** 904 (1989).
8. Went, G. T., Oyama, S. T., and Bell, A. T., *J. Phys. Chem.* **94,** 4240 (1990).
9. Deo, G., and Wachs, I. E., *J. Phys. Chem.* **95,** 5889 (1991).
10. Nag, N. K., and Massoth, F. E., *J. Catal.* **124,** 127 (1990).
11. Chary, K. V. R., Venkat Rao, V., and Mastikhin, V. M., *J. Chem. Soc. Chem. Commun.* 102 (1989).
12. Yoshida, S., Tanaka, T., Nishimura, Y., and Funabiki, T., *in* "Proceedings, 9th International Congress on Catalysis, Calgary, 1988" (M. J. Phillips and M. Ternan, Eds.), Vol. III, p. 1473. Chem. Institute of Canada, Ottawa, 1988.
13. Sobalik, Z., Lapina, O. B., and Mastikhin, V. M., *in* "Preparation of Catalysts V" (G. Poncelet, P. A. Jacobs, P. Grange, and B. Delmon, Eds.), p. 507, Studies in Surface Science and Catalysis, Vol. 63. Elsevier, Amsterdam, 1991.
14. Hönicke, D., Mitzel, H., and Xu, J., *Chem. Ing. Tech.* **62,** 940 (1990).
15. Stobbe-Kreemers, A. W., Soede, M., Veenman, J. W., and Scholten, J. J. F., *in* "Proceedings, 10th International Congress on Catalysis, Budapest, 1992" (L. Guczi, F. Solymosi, and P. Tétényi, Eds.), Vol. C, p. 1971. Akadémiai Kiadó, Budapest, 1993.
16. Brongersma, H. H., and van Leerdam, G. C., *in* "Fundamental Aspects of Heterogeneous Catalysis Studied by Particle Beams" (H. H. Brongersma and R. A. van Santen, Eds.), NATO-ASI series B 265, p. 283, Plenum, New York, 1991; Brongersma H. H., and Jacobs, J.-P., *Appl. Surf. Sci.*, **73,** 133 (1994).
17. Walden, G. H., Jr., Hammet, L. P., and Edmonds, S. M., *J. Am. Chem. Soc.* **56,** 57 (1934).
18. Noh, J. S., and Schwarz, J. A., *J. Colloid Interface Sci.* **130,** 157 (1989).
19. Broekhoff, J. C. P., Ph.D. thesis, Delft University of Technology, 1969; Parra Soto, J. B., and Otero Areán, C., *Comp. Chem.* **10,** 27 (1986).
20. Brongersma, H. H., Hazewindus, N., van Nieuwland, J. M., Otten, A. M. M., and Smets, A. J., *Rev. Sci. Instrum.* **49,** 707 (1978).
21. Le Coustumier, L. R., Taouk, B., Le Meur, M., Payen, E., Guelton, M., and Grimblot, J., *J. Phys. Chem.* **92,** 1230 (1988).
22. Lapina, O. B., Mastikhin, V. M., Simonova, L. G., and Bulgakova, Yu O., *J. Mol. Catal.* **69,** 61 (1991).
23. Baes, C. F., and Mesmer, R. E., *in* "The Hydrolysis of Cations," p. 210. Wiley, New York, 1976.
24. Li, W., and Hall, K. W., *J. Catal.* **77,** 232 (1982).
25. Ahmed, S. M., *J. Phys. Chem.* **73,** 3546 (1969).
26. Lippens, B. C., and Steggerda, J. J., *in* "Physical and Chemical Aspects of Adsorbents and Catalysts" (B. G. Linsen, Ed.), p. 171. Academic Press, New York, 1970.
27. Knözinger, H., and Ratnasamy, P., *Catal. Rev. Sci. Eng.* **17,** 31 (1978).
28. Peri, J. B., *J. Phys. Chem.* **69,** 220 (1965).
29. Van Leerdam, G. C., Ph.D. thesis, Eindhoven University of Technology, 1991.
30. Jacobs, J.-P., Maltha, A., Reintjes, J. G. H., Drimal, J., Ponec, V., and Brongersma, H. H., *J. Catal.* **147,** 294 (1994).
31. Nowińska, K., and Więckowski, A. B., *Z. Phys. Chem.* **162,** 231 (1989).
32. Bergeret, G., Gallezot, P., Chary, K. V. R., Rao, B. R., and Subrahmanyam, V. S., *Appl. Catal.* **40,** 191 (1988).
33. Eberhardt, M. A., Houalla, M., and Hercules, D. M., *SIA Surf. Interface Anal.* **20,** 766 (1993).
34. Bonné, R., Ph.D. thesis, Chap. 6, University of Amsterdam, 1992.